POLARIZATION ANISOTROPY OF LIGHT MULTIPLY BACKSCATTERED ON SPHERICAL PARTICLES

B.V. Kaul'

Institute of Atmospheric Optics,
Siberian Branch of the Russian Academy of Sciences, Tomsk
Received March 23, 1995

A mathematical description is presented for the brightness pattern in the image plane produced by radiation incident on a receiving objective due to scattering by spherical particles irradiated by a narrow beam of linearly polarized radiation. Images formed by scattered radiation passed alternately through a polarizer with orthogonal planes of polarization are essentially different and anisotropic in azimuth. This phenomenon was first discovered experimentally by Canadian researchers Carswell and Pal and is adequately described by the formula derived here. The description is given for a stationary source of light in the double-scattering approximation.

1. The anisotropy of the intensity distribution in the image of an ensemble of spherical scattering particles produced by backscattered radiation passed through a linear polarizer was first pointed out experimentally by Pal and Carswell.[1] A linearly polarized beam was used to irradiate polystyrene spherical suspension; the backscattered radiation was transmitted through a polarizer, with the transmission axis being oriented either parallel or perpendicular to the vector of electric field in the initial incident beam, and the image of a backscattering volume was then produced. The resultant images so produced have patterns displayed in Fig. 2*a*. In Ref. 1 and succeeding Ref. 2, a qualitative explanation for the phenomenon observed was given as a result of multiple scattering being affected by the specific features of single scattering of polarized radiation on spherical particles. However, Pal and Carswell proposed no mathematical description for the brightness distribution in the image plane, whereby the phenomenon being studied could be interpreted in terms of the parameters relating the observed brightness patterns with the characteristics of a scattering medium.

Below we present such mathematical description, although extremely simplified, which nevertheless encompasses the salient features of the phenomenon observed in Ref. 1.

2. In the paper, we use terms and normalization introduced in Ref. 3. For instance, the Stokes vector for radiation scattered by a volume scattering element dv in a direction φ counted off from the wave vector $\mathbf{k}_0$ of incident radiation (in the plane in which the wave vectors of incident and scattered radiation lie) at a distance R from the scattering volume is described by the equation

$$F\,\mathbf{s} = R^{-2}\,F_0\,\beta\,\mathbf{P}(\varphi)\,\mathbf{s}_0\,dv\,, \qquad (1)$$

where F_0 and F have meanings of the incident and scattered flux through unit surface area within unit solid angle, β is the volume scattering coefficient, and $\mathbf{s}_0$ and $\mathbf{s}$ are the dimensionless Stokes vectors scaled to the intensity and having the form

$$\mathbf{s} = (I_1,\, I_2,\, U,\, V)^{\mathrm{T}}\,, \qquad (2)$$

where the transposition symbol T indicates that $\mathbf{s}$ is the column vector.

In this presentation, I_1 and I_2 have meanings of two cross-polarized components of radiation scaled to the total intensity, that is, $I_1 + I_2 = 1$.

With Stokes vector defined by Eq. (2), the scattering phase matrix for spherical particles assumes the form

$$\mathbf{P}(\varphi) = \frac{1}{4\pi}\begin{pmatrix} P_1'(\varphi) & 0 & 0 & 0 \\ 0 & P_2'(\varphi) & 0 & 0 \\ 0 & 0 & P_3'(\varphi) & P_4'(\varphi) \\ 0 & 0 & -P_4'(\varphi) & P_3'(\varphi) \end{pmatrix}. \qquad (3)$$

In this case, the half–sum $[P_1' + P_2']/2$ represents the scattering phase function, since

$$\frac{1}{2}\oint [P_1'(\varphi) + P_2'(\varphi)]\,d\omega = 4\pi.$$

Equation (1) is written on the assumption that vectors $\mathbf{s}_0$ and $\mathbf{s}$ are defined in coordinate systems referred to the scattering plane, i.e., to the plane containing both vectors $\mathbf{k}$ and $\mathbf{k}_0$.

When the scattering plane is rotated about the direction of radiation propagation through an angle ψ relative to the coordinate system in which the Stokes vector of incident radiation is defined, this last must be

0235-6880/95/10 772-04 $02.00

transformed to new coordinate system referred to the scattering plane. The transformation operator for the Stokes vector in the form of Eq. (2) is

$$\mathbf{K}(\psi) = \begin{pmatrix} \cos^2\psi & \sin^2\psi & 1/2\,\sin 2\psi & 0 \\ \sin^2\psi & \cos^2\psi & -1/2\,\sin 2\psi & 0 \\ -\sin 2\psi & \sin 2\psi & \cos 2\psi & 0 \\ 0 & 0 & 0 & 1 \end{pmatrix}. \qquad (4)$$

The inverse operator follows by replacing ψ by $-\psi$. The angle ψ is considered to be positive for rotation in the counterclockwise direction when viewed in the direction counter to that of incident radiation.

3. Expressions for brightness of the image of a scattering volume can be derived in the double-scattering approximation following a scheme used in Ref. 4 to derive the equation of laser sensing. Specifically, scattering is assumed to occur in a semi-infinite layer the distance to which is much longer than the depth of radiation penetration into the layer. This means that the image of the scattering volume can all be seen by a small–angle aperture of a receiving antenna. The calculation scheme and the notation used are explained in Fig. 1.

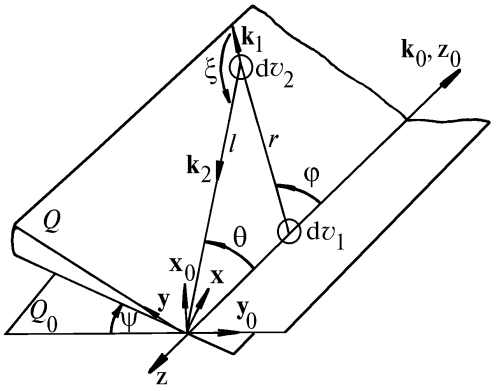

FIG. 1. Scheme of calculating the Stokes vector of doubly scattered radiation: $\mathbf{x}_0, \mathbf{y}_0, \mathbf{z}_0$ *are the unit vectors of measurement basis referred to the reference plane* Q_0; $\mathbf{k}_0$, $\mathbf{k}_1$, and $\mathbf{k}_2$ *are the wave vectors of incident, singly and doubly scattered radiation, respectively;* $\mathbf{x}, \mathbf{y}, \mathbf{z}$ *are the unit vectors of basis referred to the reference plane* Q; dv_1 *and* φ *are the volume scattering element and the scattering angles of singly scattered radiation, respectively;* dv_2 *and* ξ are the *same but for doubly scattered radiation; and,* θ *and* ψ *are the polar and azimuth angles of arrival of doubly scattered radiation, respectively.*

A laser is located at the origin of coordinates. Its radiation is propagated along the z axis. At a distance Z_0, a uniform semi-infinite scattering medium is located. Scattering and attenuation of radiation on a path $[0, Z_0]$ are neglected. The Stokes vector of laser radiation is defined in coordinate system (x_0, y_0, z_0) (Fig. 1), whose x_0 axis is chosen so as to coincide with the direction of vibration of vector $\mathbf{E}$. Hence we have

$$\mathbf{s}_0 = \{1, 0, 0, 0\}^{\mathrm{T}}.$$

Single and double scattering events are described in plane Q, rotated about the z axis through an arbitrary angle ψ with respect to the reference plane Q_0. So in new coordinate system (x, y, z) the Stokes vector is defined by the transformation

$$\mathbf{s}_0' = \mathbf{K}(\psi)\,\mathbf{s}_0, \qquad (6)$$

where $\mathbf{K}(\psi)$ is the operator given by Eq. (4), and the angle is counted off from the normal to the Q_0 plane, i.e., from the x_0 axis. Now we write down the elementary flux due to the first–order scattering by a volume scattering element dv_1 of extent dz in a direction φ and the elementary flux due to the second–order scattering by a volume scattering element dv_2 of extent dl in a direction θ caused by it (scattering angle $\xi = \pi - \varphi + \theta$). Next, integration over z and l yields the net flux arriving at a receiver objective within the solid angle $\Delta\psi\Delta\theta$. Then, the Stokes vector must be transformed to coordinate system referred to the Q_0 plane in which the measurement basis is defined. Now, since z and y axes are inverted, the operator $\mathbf{K}(\psi)$, rather than the inverse operator $\mathbf{K}(-\psi)$, must be applied again. Trajectory sections of incident and scattered beam are related as:

$$r = \frac{z\,\theta}{\sin(\varphi - \theta)}, \qquad l = \frac{z\,\sin\varphi}{\sin(\varphi - \theta)}, \qquad (7)$$

considering that $\sin\theta \approx \theta$.

According to Eq. (1), the radiation incident at the volume scattering element

$$dv_2 = l^2\,\theta\,\Delta\theta\,\Delta\psi\,dl = z^3 \sin^2\varphi\,\sin^{-4}(\varphi - \theta)\,\theta^2 \Delta\theta\,\Delta\psi\,d\varphi \qquad (8)$$

with θ_0 being the half–angle of laser beam divergence, which was scattered by the volume scattering element

$$dv_1 = \pi\,\theta_0^2\,z^2\,dz, \qquad (9)$$

has the Stokes vector $dF_1\mathbf{s}_1$ such that

$$dF_1 = \Phi_0\,\beta\,z^{-2}\,\theta^{-2}\sin^2(\varphi - \theta) \times$$
$$\times \exp\{-\beta(z - Z_0) - \beta\,z\,\theta\,\sin(\varphi - \theta)\}\,dz$$

and

$$\mathbf{s}_1 = \mathbf{P}(\varphi)\,\mathbf{K}(\psi)\,\mathbf{s}_0, \qquad (10)$$

where Φ_0 is the laser radiation power.

The elementary flux given by Eq. (10) is incident on the volume scattering element given by Eq. (8) and produces at the origin of coordinates the doubly scattered flux

$$d^2F_2\,\mathbf{s}_2 = \Phi_0\,\beta^2\,z^{-1}\,\mathbf{P}(\xi)\,\mathbf{P}(\varphi)\,\mathbf{K}(\psi)\,\mathbf{s}_0\,\Delta\theta\Delta\psi \times$$
$$\times \exp\left\{-\frac{\beta(z - Z_0)\sin\varphi}{\sin(\varphi - \theta)} - \frac{\beta\,z\,\theta}{\sin(\varphi - \theta)}\right\} d\varphi\,dz, \qquad (11)$$

where $\mathbf{P}(\xi) = \mathbf{P}(\pi - \varphi + \theta)$.

Then, upon integrating Eq. (11) over φ and z and applying again the operator $\mathbf{K}(\psi)$, we derive the Stokes vector in the reference coordinate system as a function of θ and ψ, namely

$$F_2 \mathbf{s}_2 = \Phi_0 \beta^2 \Delta\theta \, \Delta\psi \times$$
$$\times \int_{Z_0}^{\infty} z^{-1} \exp[-\beta(z - Z_0)] \; \mathbf{K}(\psi) \, \mathbf{f}(z, \theta) \, \mathbf{K}(\psi) \, \mathbf{s}_0 \, dz \; , \quad (12)$$

where

$$\mathbf{f} = \int_{\theta}^{\alpha} \mathbf{P}(\xi) \, \mathbf{P}(\varphi) \exp\left\{ - \frac{\beta \, z \, \theta}{\sin(\varphi - \theta)} - \frac{\beta(z - Z_0) \sin\varphi}{\sin(\varphi - \theta)} \right\} d\varphi \quad (13)$$

and $\alpha = \arctan z\theta/(z - Z_0)$.

The exponential terms in integrand of Eq. (13) represent the weighting functions of the trajectories. The trajectories with $\varphi < \theta$ will produce no second-order scattering in the direction θ. Also negligibly contributing will be those trajectories for which $\sin(\varphi - \theta) \ll \beta z \theta$. Quantitatively, this means that the radiation coming from the periphery of the scattering volume and concentrated within the fast varying forward peak of scattering phase function contributes insignificantly to the image intensity, while being crucial in the scattering in directions confined to scattering angles of the order of $\pi\theta_0^2/4$, where θ_0 is the half–angle of laser beam divergence. For these scattering angles, the intensity is estimated in two-stream approximation and is given by the formula

$$F_2(0) = \Phi_0 \beta^2 \mathbf{P}(\pi) \; \mathbf{P}(0) \exp(2 \beta Z_0) \; [\mathrm{Ei}_1 - \mathrm{Ei}_2] \; , \quad (14)$$

where Ei_1 and Ei_2 are the integral exponents of the first and second orders of the argument $2\beta Z_0$.

Analysis of the above relations yields the following approximation obtained by joining the asymptotic solutions for $\varphi \to 0$ and $\varphi \to \pi/2$:

$$F_2(\theta, \psi) \; \mathbf{s}_2 = \Phi_0 \, \beta \, Z_0^{-1} \{ \mathbf{P}(\pi) \; \mathbf{P}(0) \; \mathbf{s}_0 \exp(-\theta^2/\theta_0^2) +$$
$$+ \mathbf{K}(\psi) \overline{\mathbf{f}} \; \mathbf{K}(\psi) \; \mathbf{s}_0 \, [\exp(-\beta Z_0 |\theta|) - \exp(-\theta^2/\theta_0^2)] \} \; , \quad (15)$$

where $\mathbf{f}$ is the matrix with the elements

$$\overline{f}_{11} = \overline{P_1(\xi) \; P_1(\varphi)} \; , \; \overline{f}_{22} = \overline{P_2(\xi) \; P_2(\varphi)} \; ,$$

$$\overline{f}_{33} = \overline{f}_{44} = \overline{P_3(\xi) \; P_3(\varphi) - P_4(\xi) \; P_4(\varphi)} \; ,$$

$$\overline{f}_{43} = - \overline{f}_{34} = \overline{P_3(\xi) \; P_4(\varphi) + P_4(\xi) \; P_3(\varphi)} \; .$$

The other matrix elements are zeros. The bar atop indicates that the elements of the matrix $\mathbf{f}$ are obtained by integration of above products with weighting factors given by Eq. (13). We recall that $\xi = \pi - \varphi + \theta$.

By multiplying Eq. (15) by the area A of a receiving objective and dividing it by the area $\sigma = b^2 \theta \, \Delta\theta \, \Delta\psi$ in the image plane, with b being the objective focal distance, we obtain

$$F_2'(\theta, \psi) \; \mathbf{s}_2' = A \, b^{-2} \, \theta^{-1} \, F_2(\theta, \psi) \; \mathbf{s}_2 \; ,$$

which represents the Stokes vector of doubly scattered radiation in the image space.

As is obvious from Eq. (15), doubly scattered radiation consists of two flux components, one of which has the maximum intensity at the image center, rapidly decaying to its periphery, and the same polarization as the radiation incident on a scattering medium.

Polarization components on the periphery of the image are described by the following formulae:

$$I_{\perp}(d, \psi) = \frac{\Phi_0 \, \beta \, A}{Z_0 \, b \, d} \, W(d) \times$$
$$\times \left[\overline{f}_{11} \cos^4\psi + \overline{f}_{22} \sin^4\psi - \frac{1}{2} \, \overline{f}_{33} \sin^2 2\psi \right] \; , \quad (16)$$

$$I_{\perp}(d, \psi) = \frac{\Phi_0 \, \beta \, A}{Z_0 \, b \, d} \, W(d) \times$$
$$\times \left[\overline{f}_{11} + \overline{f}_{22} + \overline{f}_{33} / 2 \right] \sin^2 2\psi \; , \quad (17)$$

where

$$W(d) = [\exp(-\beta' \, d) - \exp(-d^2/d_0^2)] \; ,$$

$$\beta' = Z_0 \, \beta / b \; , \; d = |\theta| \; b \; , \; d_0 = \theta_0 \, b \; .$$

4. Now let us analyze the brightness patterns described by the formulae just obtained. Equation (17) is simplest, as it never changes its form: the product of the function $d = |\theta| b$, symmetrical about the center, and the function $\sin^2 2\psi$. Given any intensity at the center, intensity contour lines will have the patterns displayed in Fig. 2. Qualitatively, such an intensity pattern for the cross-polarized component in the image plane agrees with all the cases reported in Ref. 1.

Using formula (17), the maximum diameter of the image (at $\psi = (2n + 1)\pi/4$, $n = 0, 1, 2\ldots$) can be related with the scattering coefficient of a medium. Indeed, assuming the image edge to be at a distance d_{m} from the center, where the intensity is decreased to 7% of its maximum, we obtain

$$b = 2 \, b / d_{\mathrm{m}} \, Z_0 \; . \quad (18)$$

The image brightness distribution for the parallel component given by Eq. (16) shows more complicated pattern and depends on the size of scattering spheres. This dependence was experimentally manifested in Ref. 1 through different image diameters along x and y axes. The image diameter along the x axis is shown to coincide with that along the y axis for large-sized particles (with radii larger than 1 μm) and to be smaller than that for smaller particles. We recall that, according to the scheme adopted here, the x axis coincides with the direction of vibration of the electric vector of sounding radiation. From Eq. (16), ratio of

brightness at $\psi = 0$ (along the x axis) to that at $\psi = \pi/2$ (y axis) is

$$I_{||}(\theta, 0)/I(\theta, \pi/2) = \overline{f}_{11}/\overline{f}_{22} .$$

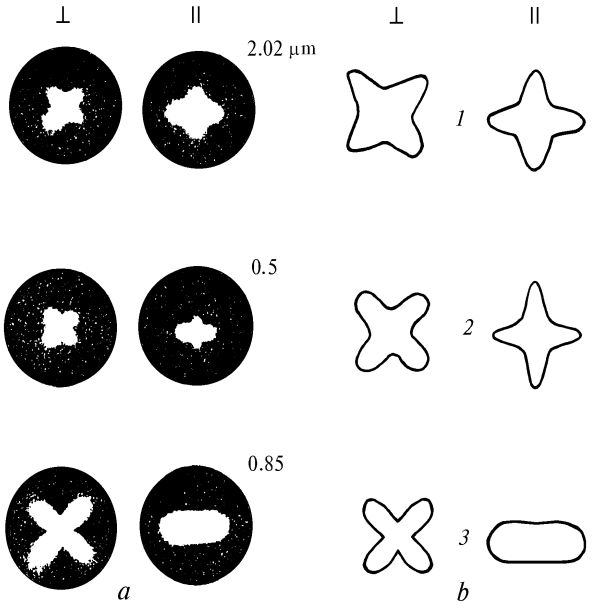

FIG. 2. Brightness patterns of multiply backscattered radiation in the plane of a receiving objective: symbols ′ and ⌈ denote normal and tangent components of linearly polarized radiation (directed vertically in the figure plane) from a source, respectively. Experimental results obtained in Ref. 1 for laser radiation (at $\lambda = 0.63$ μm*) incident on water suspension of polystyrene spherical particles with diameters indicated in the figure (a), calculation in the double–scattering approximation (b). The contour line shows the patterns of the intensity at* 0.1 *of its maximum calculated for scattering phase matrix of spherical water droplets for Deirmendjian's* C3 *cloud*[3] *(with* $d = 4$ μm*) (1), of droplets for haze* H *model*[3] *(with* $d = 0.2$ μm*) (2), and for the Rayleigh scattering phase matrix at wavelength* $\lambda = 0.7$ μm *(3).*

An estimate made for an ensemble of water–droplet spheres for Deirmendjian's to C3 cloud model[3] (with a modal radius of 2 μm) shows that $f_{11} = f_{22}$, and the resulting brightness pattern corresponds to those reported in Ref. 1 for spherical particles 2.02 and 6.08 μm in diameter.

For the Rayleigh scattering phase matrix, $\overline{f}_{11}/\overline{f}_{22} = 1/4$, and, thus, the image size along the x axis is much smaller than that along the y axis. Brightness distribution corresponds to that of Ref. 1 for scattering by water suspension of polystyrene spherical particles 0.085 μm in diameter. All the other cases considered in Ref. 1 are intermediate. However, the smaller-sized spheres unnecessarily imply the decrease of the image diameter along the x axis as compared with that along the y axis. For water droplet haze H model, for example, $f_{11} > f_{22}$, so that the image size along the x axis is larger that along the y axis, but the asymmetry is very weakly pronounced. It is quite evident that the image pattern is influenced not only by the sphere radii, but also by the difference between the refractive indices of scattering spheres and the medium in which the spheres are suspended.

Summarizing, we note that the geometry of the experiment of Ref. 1 seemingly favored recording of doubly scattered radiation. The relations established herein offer adequate qualitative description for the observed phenomenon and relate the image parameters with those of the scattering medium. With formulas (16) and (17) being approximate, their quantitative experimental validation is desirable. It is likely that when irradiating a medium with pulsed radiation, brightness distribution in the image plane will be dynamic. For example, image edge brightening would be expected as a radiation pulse penetrates deeper into scattering medium. Integrating over time of the order of $t = 1/c\beta$, however, will likely smooth the brightness pattern and it will differ insignificantly from the stationary case. Therefore, salient features of cloud sensing revealed by Pal and Carswell[2] cannot be explained within the framework of approximation adopted here, but could be explained by significant contribution of triple scattering. There are same qualitative reasons in favor of this assumption; however, its mathematical description seems to be complicated. Undoubtedly, it is of interest that irrespective of significant contributions from the third and, possibly, fourth scattering orders, as in the case of mist,[2] the image brightness distribution remains essentially anisotropic in polarized light, though it is clear that it must approach its isotropic limit with the increase of contributions from higher scattering orders. Clearly, this phenomenon can be used for the study of disperse media, more so because recording and processing of short–exposure images are quite feasible technically.

ACKNOWLEDGMENT

The work was supported in part by Russian Fund of Fundamental Research Contract No. 93–05–9376.

REFERENCES

1. A.I. Carswell and S.R. Pal, Appl. Opt. **19**, No. 24, 4123–4126 (1980).
2. S.R. Pal and A.I. Carswell, Appl. Opt. **24**, No. 21, 3464–3471 (1985).
3. D. Deirmendjian, *Electromagnetic Scattering on Spherical Polydispersions* (American Elsevier, New York, 1969), 290 pp.
4. B.V. Kaul' and I.V. Samokhvalov, Izv. Vyssh. Uchebn. Zaved. SSSR, Ser. Fizika, No. 1, 80–85 (1976).